Microstructural and Mechanical Characterization of the Different Zones of the T91/ T22 Weldment

Rutash Mittal[1*] and Buta Singh Sidhu[2]

[1]*Department of Mechanical Engineering, Malout Institute of Management & Information Technology, Malout, Dist. Sri Muktsar Sahib-152107, Punjab, India*

[2]*Punjab Technical University, Jalandhar-Kapurthala Highway, Kapurthala-144601, Punjab, India*

E-mail: [*]rutashmittal@gmail.com

Abstract—*The ferritic steels are one of the preferred structure materials for the steam generators of power plants. Dissimilar metal weldments between ferritic boiler steel of SA213T91 (T91) and SA213T22 (T22) are largely used in the different components of boilers like heat exchangers, vessel evaporators and pressure piping of thermal power plants. The T91/T22 dissimilar metal weldment fabricated by Shielded metal arc welding (SMAW) technique is Studied with the purpose of evaluation of Heat affected zone (HAZ), Weld metal (WM) and Base metal (BM) by virtue of microstructural and mechanical characteristics. The results of as welded condition for T91 side heat affected zone depict the presence of martensitic plates along with the lamellae presence of delta ferrite. The T22 side HAZ has presence of carbides in the inter-critical structure. The highest value of micro-hardness value observed on the HAZ of T91 and T22 of the weldment is due to martensitic structure and carbide presence in these regions respectively.*

Keywords*: Dissimilar Metal Weldments, Microstructures, Welding, Micro-Hardness, XRD*

INTRODUCTION

Different industries are using ferritic steels for the heat exchanger tubes of the steam generator of power plants. Different temperature zones in boilers of power plants have different grades of ferritic steels, due to which welding of these dissimilar ferritic steels are inevitable. Dissimilar metal weldments, especially between low Cr and high Cr ferritic steels are used in a number of places in steam generator circuits [1]. The adoption of dissimilar metal weldment is based on the both technical and economical reasons, along with satisfactory service performance as well as considerable savings [2]. Ferritic steels are one of the preferred materials for steam generator circuits of thermal and nuclear power plants as being resistant to high temperature corrosion as well as moderate creep rupture strength [3]. Welding of dissimilar metals not only satisfies the service conditions, but also results in large savings in minimizing the volume of expensive materials used in the dissimilar joints[4]. Several studies have reported the investigation of microstructural changes induced near the weld interface due to joining of different materials. A detailed review of mechanical characterization and micro structural studies with reference to application of joints has also been reported by many researchers [4].

The performance of the dissimilar metal weldments, more concisely of heat affected zones of the weldments is of great importance. The dissimilar metal joints are inclined to frequent failures and these failures are generally attributed to one or more of the following reasons: (a) difference in mechanical properties across the weld joint and difference in the coefficient of thermal expansion of two metals and resulting creep at the interface, (b) general alloying problems of the two different base metals such as brittle phase formation and dilution, (c) carbon migration from one side of steel into other side of steel, (d) preferential oxidation at the interface, (e) residual stresses present in the weld joints, (f) service conditions and other factors [5]. Creep rupture strength of HAZ of the 2.25Cr-1Mo steel is reported to be inferior to BM and weld metal [6].The microstructural variations caused by welding are believed to be responsible for the changes in the mechanical properties of the weldments [7]. Micro structurally altered and inhomogeneous HAZ in the weldment of 2.25Cr-1Mo steel has been observed by Raman and Gnanamoorthy [6]. The use of proper welding electrode/ filler material and welding system is a very important issue in the joining of dissimilar metals [7, 8].

Morphologies and distribution of different precipitates of the HAZ, base metal and weld metal of Cr-Mo steels have been reported by Bhaduri *et al.* [9] and Raman & Tyagi [10]. The precipitates seen in the HAZ are parallelepiped or rod shaped M_7C_3 or $M_{23}C_6$ carbides. The formation of four different regions, namely coarse grained martensite with delta ferrite, coarse grain martensite, fine grained martensite and intercritical structure are observed by Laha *et al.* [11]. Cao *et al.* [12] have studied the microstructural evolution and mechanical properties of weldment of T92 and S304 metals. The authors observed weak tensile strength of T92 CGHAZ, which is observed due to the coarse tempered martensite structure.

The available information about the structures of dissimilar weldment of SA213T91 (T91) and SA213T22 (T22) in as welded condition is scanty. In the present research, an attempt has been made to investigate the microstructures and mechanical characterization features of the dissimilar metal weldments of T91/T22 in as welded condition. Various characterization techniques like optical microscopy, X-Ray diffraction (XRD) analysis, scanning electron microscopy (SEM)/ Energy dispersive spectroscopy (EDS) are used to study the observations.

EXPERIMENTAL PROCEDURES

Base Materials and Welding Processes

The pipes of SA213T91 (T91) and SA213T22 (T22) of dimensions 50.5mm (O.D.) x 5.59mm (thickness) are machined to make V joint geometry having a root gap as 2mm and included angle of 75° for welding joint with SMAW welding process as depicted in Fig. 1. SA213T91 is from 9Cr-1Mo ferritic steel category and SA213T22 belong to 2.25Cr-1Mo steel family. The chemical composition of base metals and welding electrode is reported in Table 1. The details of Specifications of welding process and welding electrode are listed in Table 2.

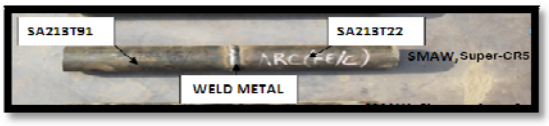

Fig. 1: Dissimilar Weldment of T91/T22, SMAW

Characterization of the Weldment

Microstructures of various zones at different magnifications are seen by using an optical microscope of Leica DM4000M at IIT Ropar, India. Standard metallographic procedure is adopted for obtaining the microstructures. The microstructures of T22 BM and T22 HAZ are examined by 5% Nital reagent {HNO_3 (5ml) + ethyl alcohol (100ml)} and of the T91, its HAZ and weld metal are treated with {$CuCl_2$ (5g) +HCl (40ml) +ethyl alcohol (25ml) +distilled water (30ml)}. The micro-hardness of different sections of the weldment is carried out using Vickers's micro-hardness tester of Wilson Instrument (an Instron company, Model No.402MVD) make at the regular interval of 0.5mm across the width of the sample. Scanning electron microscope (SEM) of JEOL Japan make having model JSM-6610LV equipped with EDS of Oxford instruments facility is used to study the microscopic modes of the samples. PAN Alytical, Model X'Pert PROMPD made in Neitherland is used to perform XRD of the specimen. Instead of the general XRD scan of the whole weldment [13], specific XRD scan of the specific section i.e. HAZ, WM etc. is performed for the specific information about the phases.

RESULTS AND DISCUSSION

Microscopic Studies of the Weldment in as Welded Condition

The evolution of optical microstructure of the weldment is presented in Fig. 2(a) to (q) at the important sections along the weldment. Fig. 2(a) depicts the optical microstructure of T91 BM. The interference from T91 BM to T91 HAZ presented in Fig. 2(b) and (c) depicts a clear effect of thermal cycles of welding on the HAZ.

Table 1: Chemical Composition of Base Metals and Welding Electrode

Base Material/ Welding Electrode	C	Cr	Mn	Mo	Si	V	Fe
SA213T91	0.0964	8.76	0.478	1.03	0.37	0.26	balance
SA213T22	0.1277	2.012	0.69	0.83	0.37	-	balance
Super-CR5	0.06	5.20	0.9	0.5	0.4	-	balance

Table 2: Details of Welding Process and Welding Electrode

S. No.	Welding Process Used	Specification of Welding Electrode Used	Applied Voltage and Current	Polarity and Number of Passes
1	SMAW (shielded metal arc welding)	Super-CR5 (D&H Secheron), AWS :E-8018-B6 3.15mm dia. electrode	Root Run: V=15V, I=100 amp. Subsequent passes: V=15V, I=130 amp.	D.C.E.N., three

The micro mechanism responsible for the formation of martensite structure on T91 HAZ depends on the peak temperature attained and cooling rate of that specified region. Depending on the temperature of HAZ to be above AC3 or above AC1 (i.e. between AC1 and AC3), austenitic or a mixture of ferritic and austenitic structure gets formed which on cooling gets transformed into the martensitic structure.

The microstructures of the T91 HAZ are segregated into two zones, namely fine grained heat affected zone (FGHAZ) and coarse grained heat affected zone (CGHAZ) as shown in Fig. 2 (d), (e) and (f). The CGHAZ is just adjacent to the weld metal with a martensitic structure having large grain size, where as FGHAZ just after the T91 BM is having lesser grain size. The optical microstructure of CGHAZ in Fig. 2(f) depicts the plate like structure of martensite having the presence of delta ferrite which is produced above AC4 temperature range. Presence of delta ferrite in CGHAZ, similar to martensite laths in size and shape and is observed to be sandwiched between martensitic laths. Different regions of the HAZ have different morphologies of microstructure. The complex formation of segregated microstructures depends on the peak temperature experienced during welding, details of the phase diagram, grain growth characteristics and continuous cooling transformation diagram [14]. The identical findings regarding carbide precipitation have also been reported [6, 10, and 15] in HAZs during research on welding of steels. The SEM micrographs of the weldment at different sections of interest are presented in Fig. 3(a) to (d). The SEM micrograph depicting the transition from T91 BM to T91 HAZ shown in Fig. 3(a), where as detailed information available in Table 3 and Table 4 presents an increase in the composition of Cr in the T91 HAZ region. Fe and Cr in the T91 HAZ combine with carbon to form the carbides of $(Cr, Fe)_3C_3$,Cr_3C_3 and Fe_3C verified by the particular XRD scan of the T91 HAZ shown in Fig. 4. The well bonded interface of T91 HAZ

with the weld metal is clearly visible in the optical microstructure of Fig. 2(g) and (h) and SEM micrograph of Fig. 3(b). The optical microstructure of weld metal shown in Fig. 2(i) and (j) depicts a cast weld structure having high micro-hardness. The acicular morphology of ferrite and austenite is being observed in the microstructure of the weld metal. While moving from weld metal towards the T22 base metal, the microstructure of T22 HAZ is encountered having a bainitic structure in the HAZ just adjacent to the weld metal. The structure of T22 HAZ at various important places is presented in Fig. 2(l), (m) and (n). An inter-critical region in the T22 HAZ adjacent to T22 BM has been observed, having the presence of carbides [16, 17]. The carbides of $(Cr, Fe)_3C_3$ and Cr_3C_3, shown in Fig. 2(n) and (o) are distributed in the polygonal phases of ferrite and pearlite. Additionally, phases of Fe_2Mo and intermetallics of Ni-Cr-Fe and FeNi have also been observed in particular XRD scan of T22 HAZ in Fig. 4. The SEM micrographs of the weld metal and the interface of T22 HAZ/T22 BM are presented in Fig. 3(c) and (d). As per Fig. 3(d) and detail information of Table 2, an increase in Cr composition is observed in the T22 HAZ, causing the formation of carbides which ultimately increases the micro-hardness of T22 HAZ [18, 19]. The heat input from welding has promoted sensitization (formation of carbides) in the HAZs, because portions of the HAZs are heated in the sensitization temperature range during slow heating or cooling through this temperature range during welding. Hence, due to the effect of sensitization the formation of carbides with high micro-hardness is observed on the HAZs of T91 and T22.

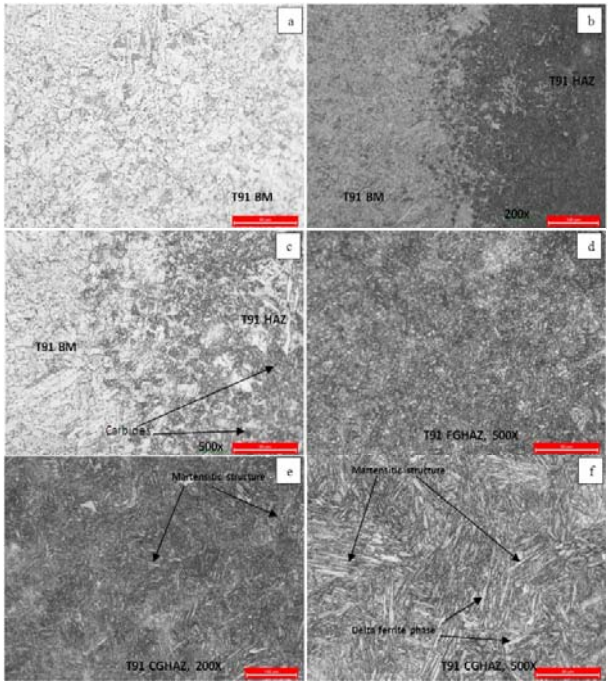

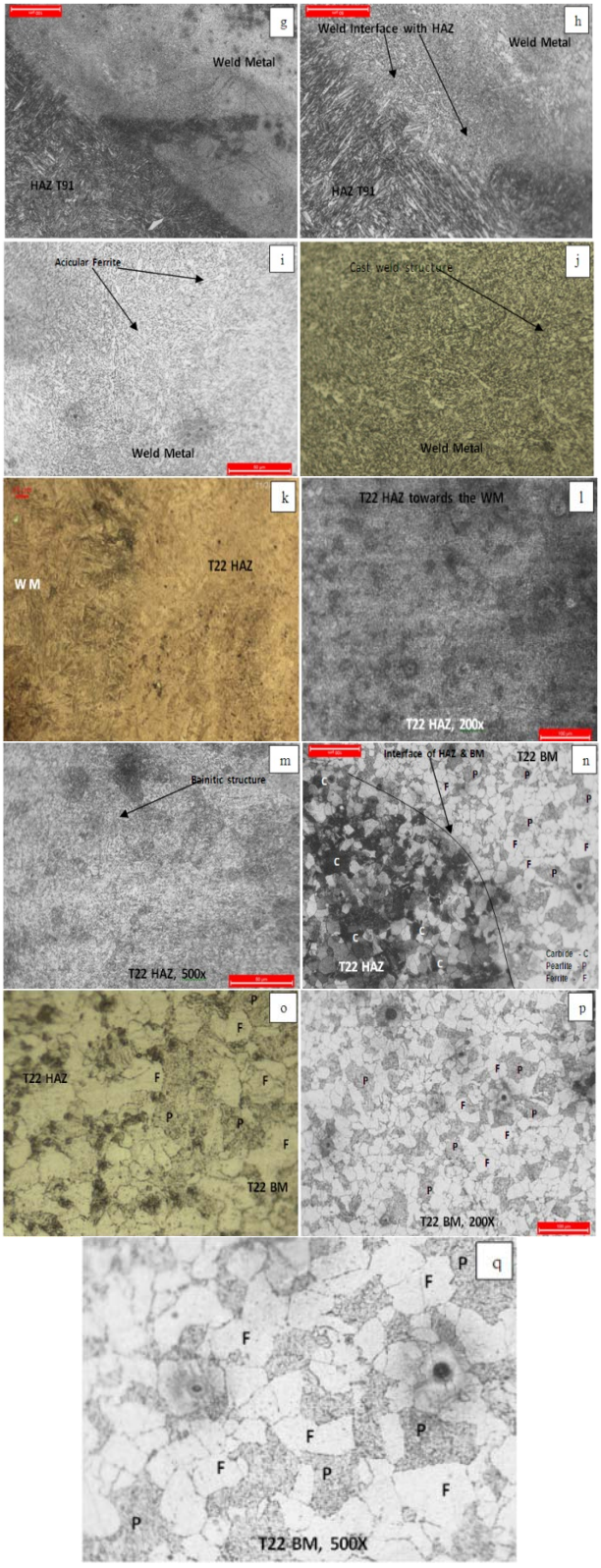

Fig. 2: Optical Microstructures of T91/T22 Weldment in as Welded Condition

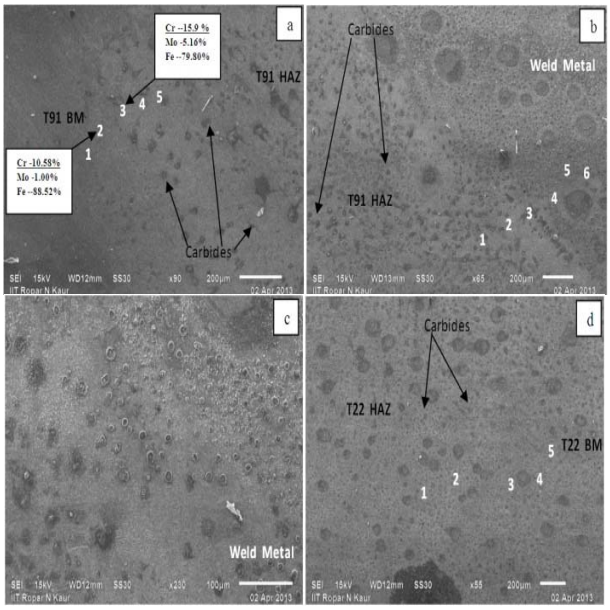

Fig. 3: SEM Micrographs of T91/T22 Weldment in as Welded Condition

Table 3: Change of Elemental Composition along T91 BM and T91 HAZ Interface

	T91 BM		T91 HAZ		
Elements	1	2	3	4	5
Cr	9.67	10.58	15.19	9.71	8.57
Fe	90.3	88.52	79.6	87.01	90.46
Mo	-	1.00	5.16	3.28	0.97

Table 4: Change of Elemental Composition along T91 HAZ and WM Interface

	T91 HAZ			WM		
Elements	1	2	3	4	5	6
Cr	10.28	9.93	-	2.24	2.66	3.58
Fe	81.93	89.41	94.02	91.0	90.2	90.18
Mo	7.79	-	5.70	5.62	7.13	2.78
Ni			0.28	1.15	-	1.55

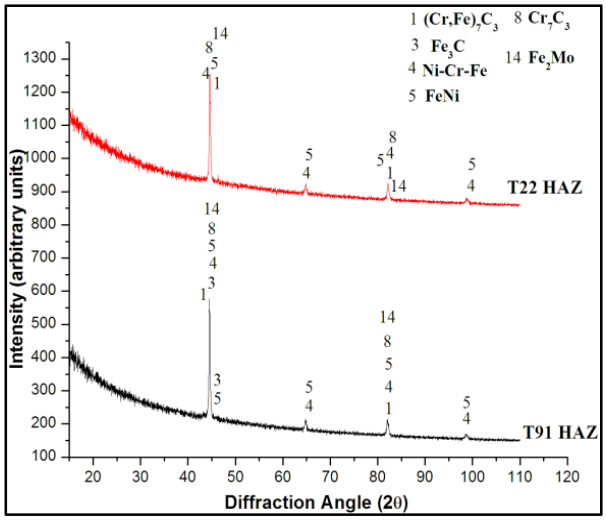

Fig. 4: XRD Patterns of Different Regions of T91/T22 Weldment

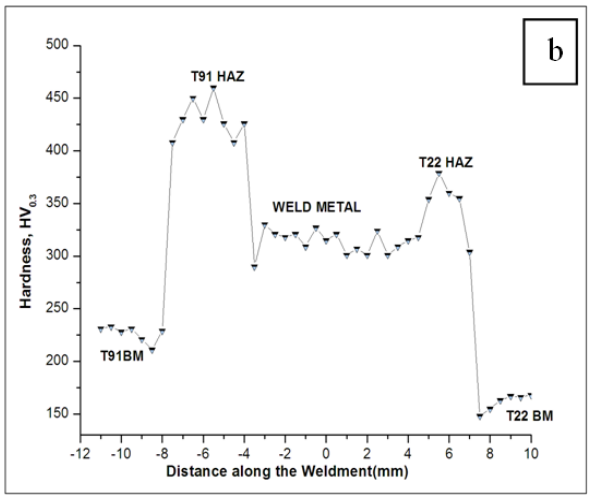

Fig. 5: Microhardness Pattern along the T91/T22 Weldment

Micro-Hardness Measurement in as Welded Condition

The profile of micro-hardness is presented in Fig. 5, which shows an increase in micro-hardness value of the T91 HAZ region. The average micro-hardness of this region is around 430Hv.The increase in micro-hardness value moving from weld metal to T91 HAZ can clearly be correlated to the optical microstructures and SEM micrographs (Fig. 2(d) and (e) & Fig. 3(a) and (b)). The observed high micro-hardness of T91 HAZ is by virtue of the presence of carbides and martensitic structure as demonstrated in Fig. 2(c). A drop in micro-hardness is observed in T91 BM just adjacent to the T91 HAZ, which may be because of transfer of carbon from base metal to HAZ due to carbon affinity towards the weld metal [13, 19]. While moving from T91 BM to weld metal, carbon does not pass to weld metal, but combines with Cr and other elements in the T91 HAZ to form carbide precipitation phases [1, 7]. The average micro-hardness of the weld metal region is around 312Hv and distribution of micro-hardness seems to be uniform throughout the weld metal region. The higher value of micro-hardness of weld metal in uniform profile can be by virtue of cast weld and acicular structure of ferrite. The weld metal region has crystallized form of filler material having micro alloyed presence of Cr, Mn, Ni and Mo, which also contributes towards increasing micro-hardness. An increase in micro-hardness is observed in the hard zone of T22 HAZ while moving from weld metal to T22 BM having an average value to be around 338Hv. Just similar to the drop in micro-hardness value on the T91 BM of the weldment a drop in micro-hardness has also observed in the T22 BM side just adjacent to T22 HAZ. This micro-hardness drop may be due to transfer of carbon from T22 BM to T22 HAZ where it seems to form carbides in the inter-critical

structure of polygonal ferrite and pearlite (Fig. 2(n)), similar to the behavior reported by researchers [6, 9 and 16]. The formation of martensitic structure on the T91 HAZ and the presence of carbides on T91 HAZ and T22 HAZ also corroborate the observations of other researchers [1, 9 and 10]. The micro-hardness distribution of the weldment is asymmetrical with respect to weld center.

CONCLUSIONS

The dissimilar metal weldment of T91/T22 is successfully prepared by SMAW process. The major conclusions of the study are:

- The variations of microstructures along the different sections of the weldment are dependable on the welding technique, thermal cycles of process, chemical composition of base metals and welding electrode.
- The higher micro-hardness of T91 HAZ side of the weldment is by virtue of the martensitic structure with lamellae presence of delta ferrite in the region.
- The higher micro-hardness of T22 HAZ side of the weldment is due to the presence of carbides and intermetalics in the inter-critical structure.
- The micro-hardness on HAZs i.e. on both sides of weld metal of all the weldments is higher than their respective base metals.

REFERENCES

[1] Sudha, C., Thomas, Paul V., Terrance, A.L.E., Saroja, S. and Vijayalakshmi, M. (2006), "Microstructure and Microchemistry of Hard Zone in Dissimilar Weldments of Cr-Mo Steels", *Welding Journal*, Vol. April, pp. 71s–80s.

[2] Sun, Z. (1996), "Feasibility of Producing Ferritic/Austenitic Dissimilar Metal Joints by High Energy Density Laser Beam Process", *International Journal of Pressure Vessel and Piping*, Vol. 94, pp. 153–160.

[3] Anand, R., Sudha, C., Thomas, Paul V., Saroja, S. and Vijayalakshmi, M. (2010), "Microstructural Changes in Grade 22 Ferritic Steel Clad Successively with Ni-based and 9 Cr Filler Metal", *Welding Journal*, Vol. 89, pp. 65s–73s.

[4] Rutash, Mittal, Lucky, Goyal and Singh, Sidhu Buta (2012), "Metallurgical Aspects of Dissimilar Metal Weldments: A Review", *Proceedings of the International Conference on Advancements and Futuristic Trends in Mechanical and Materials Engineering*, Kapurthala, Punjab, India, pp. 669–675.

[5] Joseph, A., Rai, S.K., Jayakumar, T. and Murugan, N. (2005), "Evaluation of Residual Stresses in Dissimilar Weld Joints", *International Journal of Pressure Vessel and Piping*, Vol. 82, pp. 700–705.

[6] Raman, R.K.S. and Gnanamoorthy, J.B. (1993), "The Oxidation Behavior of the Weld Metal, Heat Affected Zone and Base Metal in the Weldments of 2.25Cr-1Mo Steel", *Corrosion Science*, Vol. 34, pp. 1275–1288.

[7] Shah, Hosseini H., Shamanian, M. and Kermanpur, A. (2011), "Characterization of Microstructures and Mechanical Properties of Inconel 617/310 Stainless Steel Dissimilar Welds", *Material Characterization*, Vol. 62, pp. 383–386.

[8] Kacer, R. and Baylan, O. (2005), "An Investigation of Microstructural Property Relationships in Dissimilar Welds between Martensitic and Austenitic Stainless Steels", *Materials & Design*, Vol. 25**,** pp. 317–329.

[9] Bhaduri, A.K., Venkadesan, S., Rodrigues, P. and Mukanda, P.G. (1994), "Transition Metal Joints for Steam Generators-An Overview", *International Journal of Pressure Vessel and Piping*, Vol. 58, pp. 251–265.

[10] Raman, R.K. Singh and Tyagi, A.K., (1994), "Secondary Ion Mass Spectrometry and Surface Profilometry Characterization of Oxide Scales Developed over Various Regions of Weldments of 2.25Cr-1Mo Steel", *Material Science & Engineering A*, Vol. 85, pp. 97–102.

[11] Laha, K., Chandravathi, K.S., Rao, K.B.S. and Mannan, S.L., (1995), "Hot Tensile Properties of Simulated Heat Affected Zone Microstructures of 9Cr-1Mo Weldment", *International Journal of Pressure Vessel and Piping*, Vol. 62, pp. 303–311.

[12] Cao, J., Gongn, Y., Yang, Z., Luo, X. and Gu, F., (2011), "Microstructure and Mechanical Properties of Dissimilar Materials Joints between T91 Martensitic and S304H Austenitic Steel", *Materials & Design*, Vol. 32, pp. 2763–2770.

[13] Arivazhagan, N., Narayanan, S., Singh, S., Reddy, M. and Prakash, S. (2012), "High Temperature Corrosion Studies on Friction-Welded Low Alloy Steel and Stainless Steel in Air and Molten Salt Environment at 650°C", *Materials & Design*, Vol. 34, pp. 459–468.

[14] Kou, S.(2003), *Welding Metallurgy*, New Jersey, John Wiley & Sons, pp. 268–270.

[15] Sun, Z. (1996), "Feasibility of Producing Ferritic/austenitic Dissimilar Metal Joints by High Energy Density Laser Beam Process", *International Journal of Pressure Vessel and Piping*, Vol. 94, pp. 153–160.

[16] Sudha, C., Terrance, A.L.E., Albert, S.K. and Vijayalakshmi, M., (2000), "Systematic Study of Formation of Soft and Hard Zones in the Dissimilar Weldments of Cr-Mo Steels", *Journal of Nuclear Material*, Vol. 302, pp. 193–205.

[17] Han, Huai- yae and sun, Z. (1994), "Welding of Tube to Tube Joins between Meteoritic Austenitic Stainless Steads for Reactor Applications", *International Journal Pressure Vessel and Piping*, Vol. 60, pp. 59–64.

[18] Pilling, J. and Ridley, N. (1982), "Tempering of 2.25Pct Cr-1Pct Mo Low Carbon Steels", *Metallurgical Transactions A*, Vol. 13, pp. 557–563.

[19] Sireesha, M., Albert, Shaju K., Shankar, V. and Sundaresan, S. (2000), "Comparative Evaluation of Welding Consumables for Dissimilar Welds between 316LN Austenitic Stainless Steel and Alloy 800", *Journal of Nuclear Material*, Vol. 279, pp. 65–76.